Photophysical Characterization of a Series of Platinum(II)-Containing Phenyl−Ethynyl Oligomers

Joy E. Rogers,*,† Thomas M. Cooper,‡ Paul A. Fleitz,‡ Douglas J. Glass,† and Daniel G. McLean§

Materials and Manufacturing Directorate, Air Force Research Laboratory, 3005 P Street Ste 1 Bldg 651, Wright Patterson Air Force Base, Ohio 45433, Technical Management Concepts Inc., Dayton, Ohio 45433, and Science Applications International Corporation, Dayton, Ohio 45434

Received: May 21, 2002; In Final Form: August 20, 2002

A comprehensive photophysical study has been carried out on a series of platinum(II)-containing phenyl−ethynyl oligomers. The compounds are composed of a platinum center attached to two tributylphosphine ligands and two ligands that vary the number of repeat phenyl−ethynyl units (−Ph−C≡C−). The objective of this work is to understand the effects of increased conjugation and the influence of the platinum on the overall electronic structure of the molecule. This was done by utilizing steady-state absorption, steady-state emission, picosecond pump−probe, and nanosecond laser flash photolysis techniques. The effect of increased conjugation is a red shift of S_0-S_1 and T_1-T_n and an increase in both the S_0-S_1 and T_1-T_n molar extinction coefficients. The spin−orbit coupling effect of platinum on the ground and excited-state properties is reduced with increased conjugation length because the S_0-S_1 transition is more localized on the ligand. As the ligand becomes larger, it takes on more $\pi-\pi^*$ character and therefore is spatially further away from the platinum center.

Introduction

There has been much interest in the development of polymers for use in materials science. Specifically the field of developing π-conjugated oligomers and polymers for their electronic and optical properties has increasingly expanded.[1−3] Due to the interesting properties of π-conjugated systems, they are currently being developed for use in light emitting diodes (LED),[4,5] lasers (nonlinear optical properties),[6] and conductance switches.[7]

The incorporation of a transition metal into the polymer changes the redox, optical, and electronic properties and allows for tunability of these properties. Several reviews were recently published focusing on a variety of transition metal-containing complexes.[8−10] The above-mentioned reviews are very broad in covering a variety of systems and presenting the optical and electronic properties but very few detailed studies have been carried out concerning the effect of the metal on the π-conjugated system. Due to the complexity of the electronic properties of metal-containing systems, there is a need to study smaller well-defined systems with varying conjugation length as a means for better understanding the effects of the metal on the overall system.

One area of interest involves the study of transition metal-containing phenyl−ethynyl oligomers and polymers. A few examples of metalated systems include the study of the optical properties of nickel,[11] palladium,[12] rhenium,[13] ruthenium,[14] and platinum[15,16] phenyl−ethynyl oligomers and polymers. Although there is a wealth of information on the optical and electronic properties of these compounds, there are only a few studies that systematically look at the effects of the metal on the phenyl−ethynyl ligand. Therefore we decided to examine a well-defined system of phenyl−ethynyl oligomers.

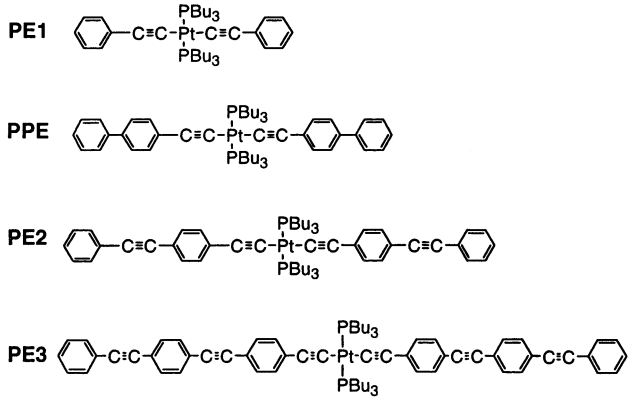

Figure 1. Shown are the structures of the platinum-containing oligomers PE1, PPE, PE2, and PE3.

To understand the structure−property relationship of these systems, a series of platinum(II)-containing oligomers with varying length ligands, composed of an increasing number of repeat phenyl−ethynyl units (−Ph−C≡C−), have been synthesized and are shown in Figure 1. In this paper we report on work that focuses on understanding the effects of increased conjugation and understanding the influence of the platinum atom on the overall electronic structure of the molecule. To understand the effects of increasing the conjugation length, we utilized various spectroscopic techniques to map out the photophysical properties of this series of oligomers. In this paper we report on various properties including molar absorption coefficients, quantum yields, and rate constants and draw conclusions based on the trends observed.

Experimental Section

Synthesis. *trans*-$Pt(PBu_3)_2Cl_2$ was prepared according to literature methods.[17] The PE3 precursor, 4-(2-(4-ethynylphenyl)-

* Corresponding author. E-mail: Joy.Rogers@wpafb.af.mil.
† Technical Management Concepts Inc.
‡ Wright Patterson Air Force Base.
§ Science Applications International Corp.

10.1021/jp021263d CCC: $22.00
Published on Web 09/28/2002

ethynyl)-1-(2-phenylethynyl)benzene, was prepared according to literature methods.[18]

PE1. *trans*-Bis(tributylphosphine)bis(ethynylphenyl)platinum was synthesized according to literature procedures.[19] IR (dried film): ν/cm^{-1} 2102 (s, Pt−CC). ^{1}H NMR ($CDCl_3$, 300 MHz): δ 7.285−2.280 (d, 4H, Ar), 7.197−7.172 (t, 4H, Ar), 7.104−7.080 (t, 2H, Ar), 2.176−2.097 (m, 12H, CH_2), 1.617−1.570 (m, 12H, CH_2), 1.557−1.381 (m, 12H, CH_2), 0.868−0.844 (t, 18H, CH_3). EIMS *m*/*z* calcd (found) for $C_{40}H_{64}P_2Pt$: M^+ *m*/*z* 802 (802). There was also a significant EIMS fragment C_6H_5−CC−$P(C_4H_9)_3$ calcd (found) for $C_{20}H_{32}P$: M^+ *m*/*z* 303 (303). UV max (benzene, 25 °C): 324 nm (ϵ = 24 700 ± 500 M^{-1} cm^{-1}).

PPE. *trans*-Bis(tributylphosphine)bis(4-ethynylbiphenyl)platinum was synthesized by the following procedure: CuI (14 mg) was added to a degassed mixture of 0.671 g (1.00 mmol) of *trans*-$Pt(PBu_3)_2Cl_2$ and 0.39 g (2.2 mmol) of diphenylacetylene dissolved in 50 mL of diethylamine. The dehydrohalogenation reaction was allowed to run overnight. The solvent was removed and the crude product was purified by column chromatography followed by recrystallization from methanol. A 50% yield was obtained. IR (dried film): ν/cm^{-1} 2100 (s, Pt−CC). ^{1}H NMR ($CDCl_3$, 300 MHz): δ 7.603−7.578 (d, 4H, Ar), 7.578−7.415 (m, 8H, Ar), 7.396−7.327 (m, 6H, Ar), 2.154 (m, 12H, CH_2), 1.626 (m, 12H, CH_2), 1.500−1.432 (m, 12H, CH_2), 0.961−0.913 (t, 18H, CH_3). EIMS calcd (found) for $C_{52}H_{72}P_2Pt$: M^+ *m*/*z* 954 (954). There was also a significant fragment C_6H_5−C_6H_4−CC−$P(C_4H_9)_3$ calcd (found) for $C_{26}H_{36}P$: M^+ *m*/*z* 379 (379). UV max (benzene, 25 °C): 332 nm (ϵ = 44 400 ± 600 M^{-1} cm^{-1}).

PE2. *trans*-Bis(tributylphosphine)bis(4-ethynyl-1-(2-phenylethynyl)benzene)platinum was synthesized according to literature procedures.[16] IR (dried film): ν/cm^{-1} 2097 (s, Pt−CC). ^{1}H NMR ($CDCl_3$, 300 MHz): δ 7.526−7.503 (m, 4H, Ar), 7.386-7.324 (m, 8H, Ar), 7.235 (m, 6H, Ar), 2.139 (m, 12H, CH_2), 1.603−1.559 (m, 12H, CH_2), 1.455−1.435 (m, 12H, CH_2), 0.946−0.899 (t, 18H, CH_3). EIMS calcd (found) for $C_{56}H_{72}P_2Pt$: M^+ *m*/*z* 1002 (1002). There was also a significant EIMS fragment C_6H_5−CC−C_6H_4−CC−$P(C_4H_9)_3$ calcd (found) for $C_{28}H_{36}P$: M^+ *m*/*z* 403 (403). UV max (benzene, 25 °C): 355 nm (ϵ = 89 000 ± 1200 M^{-1} cm^{-1}).

PE3. *trans*-Bis(tributylphosphine)bis(4-(2-(4-ethynylphenyl)-ethynyl)-1-(2-phenylethynyl)benzene)platinum was synthesized by the following procedure. CuI (10 mg) was added to a degassed mixture of 0.37 mmol (0.246 g) of *trans*-$Pt(PBu_3)_2Cl_2$ and 0.74 mmol (0.22 g) of the 4-(2-(4-ethynylphenyl)-ethynyl)-1-(2-phenylethynyl)benzene dissolved in 50 mL of diethylamine. The dehydrohalogenation reaction was allowed to run overnight. The solvent was removed and the crude product was purified by column chromatography followed by recrystallization from methanol/dichloromethane. A 42% yield was obtained. IR (dried film): ν/cm^{-1} 2092 (s Pt−CC). ^{1}H NMR ($CDCl_3$, 300 MHz): δ 7.484−7.424 (m, 14H, Ar), 7.323−7.296 (m, 8H, Ar), 7.283−7.148 (m, 4H, Ar), 2.086−2.035 (m, 12H, CH_2), 1.551−1.487 (m, 12H, CH_2), 1.413−1.341 (m, 12H, CH_2), 0.881−0.834 (t, 18H, CH_3); EIMS calcd for $C_{72}H_{80}P_2Pt$: M^+ *m*/*z* 1202. Only the parent ion breakdown fragment C_6H_5−C_6H_4−CC−C_6H_4−CC−$P(C_4H_9)_3$ calcd (found) for $C_{36}H_{40}P$: M^+ *m*/*z* 503 (503) was observed. UV max (benzene, 25 °C): 377 nm (ϵ = 85 200 ± 1800 M^{-1} cm^{-1}).

General Techniques. Ground-state UV/vis absorption spectra were measured on a temperature-controlled Cary 500 spectrophotometer and an Ocean Optics long cell spectrometer (LCS) that uses multiple cells of varying path lengths to measure molar absorption coefficients of very small transitions. Emission spectra were measured using a Perkin-Elmer model LS 50B fluorometer. Room-temperature phosphorescence spectra were obtained by purging the samples in benzene with argon prior to the measurement. All samples were excited at 350 nm to determine the fluorescence quantum yields, but spectra shown were excited at 340 nm. Low-temperature phosphorescence studies of PE1 were done using methylcyclohexane as a frozen glass at 77 K and exciting at 324 nm.

Fluorescence Quantum Yields. Fluorescence quantum yields were determined using the method of relative actinometry. Quinine sulfate was used as an actinometer with a known fluorescence quantum yield of 0.55 in 1.0 N H_2SO_4.[20] The quantum yields for the oligomers (Φ_0) were determined as shown in

$$\Phi_0 = \Phi_{QS}\frac{(A_{QS})(\eta_0^{\,2})(\Delta_O)}{(A_0)(\eta_{QS}^{\,2})(\Delta_{QS})} \qquad (1)$$

In eq 1, Φ_{QS} is the fluorescence quantum yield of quinine sulfate, η_0 and η_{QS} are the index of refraction for benzene and H_2SO_4, respectively, *A* is the absorptance (1-transmittance), and Δ is the area of the emission spectrum. All samples were excited at 350 nm with a matched optical density of 0.1.

Phosphorescence Quantum Yields. Phosphorescence quantum yields were measured at room temperature using deoxygenated samples. Oxygen was removed from each sample by three successive freeze−pump−thaw cycles. The values obtained were determined by comparing the area due to fluorescence to that due to phosphorescence. Knowing the fluorescence quantum yields determined earlier we simply used a ratio identity to determine the phosphorescence quantum yields. All samples were excited at 340 nm for this determination.

Pump−Probe Spectroscopy. Picosecond transient absorption measurements were done using a pump−probe technique to identify short-lived transients. Samples were pumped using the third-harmonic (355 nm) of a ca. 30 ps pulse from a Continuum PY61C mode-locked Nd:YAG laser. The probe pulse is generated by passing residual 1064 nm light through a continuum generator (D_2O/H_2O) and is routed through a variable delay line and arrives at the sample at varying times with respect to the pump. The pump pulse is sent to the sample along a constant fixed length line. Both reference and sample beams were coupled into separate legs of a bifurcated fiber-optic bundle and dispersed using a spectrograph/monochromator. A dual diode array was used to obtain transient spectra, and matched PMT detectors were used for single-wavelength kinetic measurements. Instrument response times are typically 30−45 ps, assuming Guassian profiles. A detailed description of the pump−probe spectroscopy apparatus has been previously published.[21]

Laser Flash Photolysis. Nanosecond transient absorption measurements used the technique of laser flash photolysis. The third harmonic (355-nm) of a Q-switched Nd:YAG laser (Continuum YG661, pulse width ca. 15 ns) is used for laser flash excitation. Pulse fluences of up to 8 mJ cm^{-2} are typically used at the excitation wavelength. Laser-induced transmittance changes are monitored using white light from a 75 W xenon source (Photon Technology International) focused through the sample, and re-imaged on the entrance slit of a Digikrom 240 monochromator. The resolved or dispersed light is detected with a Hamamatsu R-928 photomultiplier tube and the current is routed through a back-off circuit that measures and compensates for I_0, the background transmitted intensity. The real time current

is recorded across 50 ohms on a Tektronix TDS 3054 digital oscilloscope. Data were collected and analyzed using routines written in National Instruments Lab View 5.1.

Triplet Sensitization. The molar absorption coefficients of the oligomer triplet states were determined using the method of triplet sensitization. β-Carotene was utilized as a triplet energy acceptor due to its large excited-state molar absorption coefficient at 515 nm (163 000 ± 18 000 M^{-1} cm^{-1}).[22] This value is within error of the previously published value in benzene (187 000 ± 53 500 M^{-1} cm^{-1}).[23] PPE, PE2, and PE3 were directly excited using 355 nm. Direct excitation of β-carotene to form the triplet excited state was minimal due to a very small triplet quantum yield (<0.001).[24] In this experiment the β-carotene absorbs a significant portion of the incident laser light but due to the transverse pumping geometry of the cuvette holder, inner filter effects are negligible. Also the concentration of oligomer triplet excited state produced within the laser pulse was carefully monitored to ensure that it stays consistent throughout the experiment.

Upon excitation of each oligomer a growth was observed at 515 nm consistent with the production of the β-carotene triplet. The sensitized β-carotene T_1-T_n absorption, $\Delta A_{\beta C}$ extrapolated to time zero, was measured as a function of β-carotene concentration. The extinction coefficients of the oligomer triplet excited states were determined using the following expression.

$$\Delta A_{\beta C} = \Delta A_0 \frac{\Delta \epsilon_{\beta C}}{\Delta \epsilon_0} f_q \tag{2}$$

In eq 2, $\Delta A_{\beta C}$ is the measured β-carotene T_1-T_n differential absorbance change at 515 nm (extrapolated back to the time immediately following the laser pulse), $\Delta \epsilon_{\beta C}$ is the known differential molar absorption coefficient for β-carotene at 515 nm, ΔA_0 is the T_1-T_n maximum differential absorbance of the oligomer at time zero immediately following the laser pulse, and f_q is the fraction of the oligomer triplet excited states that are quenched by the β-carotene. The fraction quenched is defined in

$$f_q = \frac{k_{obs}}{k_{obs} - k_d} \tag{3}$$

In eq 3, k_{obs} is the observed rate constant in the presence of quencher (β-carotene) and k_d is the triplet-state decay constant of the oligomer without quencher. The T_1-T_n molar absorption coefficient ($\Delta \epsilon_0$) is determined by plotting $\Delta A_{\beta C}$ vs f_q with knowledge of ΔA_0.

Singlet Depletion. Calculation of the triplet excited-state molar absorption coefficients of the oligomers from the differential absorbance was also determined using the method of singlet depletion.[25] In this technique the ground-state bleaching of the T_1-T_n absorbance spectrum is compared to a ground-state molar extinction spectrum. Utilizing the known relationship in eq 4 leads to a correlation between the two molar extinction spectra.

$${}^3\epsilon_0(\lambda) = {}^1\epsilon_0(\lambda) + \frac{\Delta A_0(\lambda)}{[{}^3O^*]l} \tag{4}$$

In eq 4, ${}^3\epsilon_0(\lambda)$, and ${}^1\epsilon_0(\lambda)$ are the respective molar extinction coefficients, ΔA_0 is the difference of the T_1-T_n absorption and the ground-state absorption at a particular wavelength, l is the path length, and $[{}^3O^*]$ is the triplet excited-state concentration at the time correlating with ΔA_0. In this technique the triplet excited-state concentration is varied to find a value where the triplet excited-state spectrum shows no evidence of the peaks in the ground-state spectrum. This is done at the strongest peak by minimizing the correlation between ${}^3\epsilon_0(\lambda)$ and ${}^1\epsilon_0(\lambda)$ using Mathcad. This method requires good linearity of the detection system in measuring the negative portion of $\Delta A_0(\lambda)$ and good matching of the spectrometers measuring $\Delta A_0(\lambda)$ and ${}^1\epsilon_0(\lambda)$.

Intersystem Crossing Quantum Yields. Quantum yields for intersystem crossing were determined using

$$\Phi_{ISC} = \frac{\Delta A_0}{(\Delta \epsilon_0)[O^*]_0 b} \tag{5}$$

In eq 5, ΔA_0 is the measured absorbance change extrapolated to time zero after the laser pulse, $\Delta \epsilon_0$ is the triplet minus ground-state molar absorption coefficient of the oligomer, b is the cell path length, and $[O^*]_0$ is the total concentration of excited states at zero time, measured using a benzophenone actinometer ($\Delta \epsilon_{BP}$ = 6500 M^{-1} cm^{-1} at 520 nm).[25] Matched optical densities of the oligomers and benzophenone at 355 nm were utilized in each determination.

Phosphorescence Decay Rate Constants. Using the following equation, the phosphorescence rate constant (k_P) is determined.

$$\Phi_P = \Phi_{ISC} k_P \tau_T \tag{6}$$

In eq 6, Φ_{ISC} is the quantum yield of intersystem crossing, Φ_P is the quantum yield of phosphorescence, and τ_T is the triplet excited-state lifetime at room temperature. We determined Φ_P under deoxygenated conditions.

Results

Ground-State Absorbance. A series of oligomers were synthesized that vary the ligand phenyl−ethynyl length from one to three. Shown in Figure 1 are the structures of the four oligomers studied (PE1, PPE, PE2, and PE3). We are interested in determining the effects on the photophysical properties by increasing the conjugation length of the ligands. We previously reported on this series of compounds and found that there is little solvent effect on the ground and excited-state properties from THF to benzene.[26] Shown in Figure 2 are the ground-state spectra of each of the oligomers. As the conjugation length increases, the absorption maxima increase and are red-shifted. For PE1 (λ_{max} = 324 nm), PE2 (λ_{max} = 355 nm), and PE3 (λ_{max} = 377 nm) there is approximately a 25 nm shift with the addition of one phenyl−ethynyl unit.

Organometallic compounds often possess an enhanced spin forbidden S_0-T_1 transition, due to spin−orbit coupling from a heavy atom, in the ground-state absorption spectrum.[27] Whereas these spin forbidden transitions are generally weak for organic compounds ($\epsilon = 10^{-5}$ to 10^{-6} M^{-1} cm^{-1}), some organometallic compounds exhibit much larger extinction coefficients ($\epsilon = 10^{-2}$ to 10 M^{-1} cm^{-1}). It has been shown in the literature that PE2 has a small absorption peak at 520 nm that has been assigned as a spin-forbidden radiative transition from S_0-T_1.[28] We also investigated this phenomenon using a long cell spectrometer. In this case the concentration of the oligomers is kept low (≈1 mM) to avoid aggregation effects and the path length is varied from 0.1 to 100 cm. Shown in Figure 3 are the spectra obtained for PE1 and PE2 using a 30 cm path length along with the first derivative of the spectra. Shoulders were observed at 435 and 516 nm for PE1 and PE2, respectively. The peak observed at 516 nm for PE2 is consistent with that found by McKay and

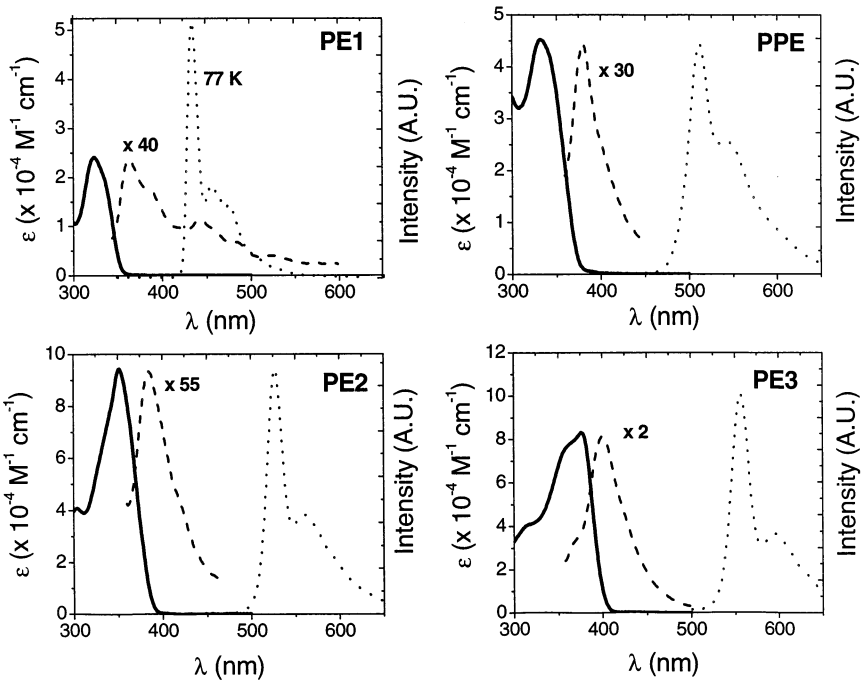

Figure 2. Ground-state absorption (solid line), fluorescence (dashed line), and phosphorescence (dotted line) of PE1, PPE, PE2, and PE3. Extinction coefficients are given for absorbance data (left axis); all others are in intensity (arbitrary units, right axis). All data were obtained at room temperature (25 °C) in benzene except the PE1 phosphorescence, which was measured at 77 K in methylcyclohexane. Samples were excited at 340 nm except for PE1, which was excited at 324 nm. Fluorescence spectra were amplified (shown on graph) relative to the intensity of the phosphorescence peak for clarity.

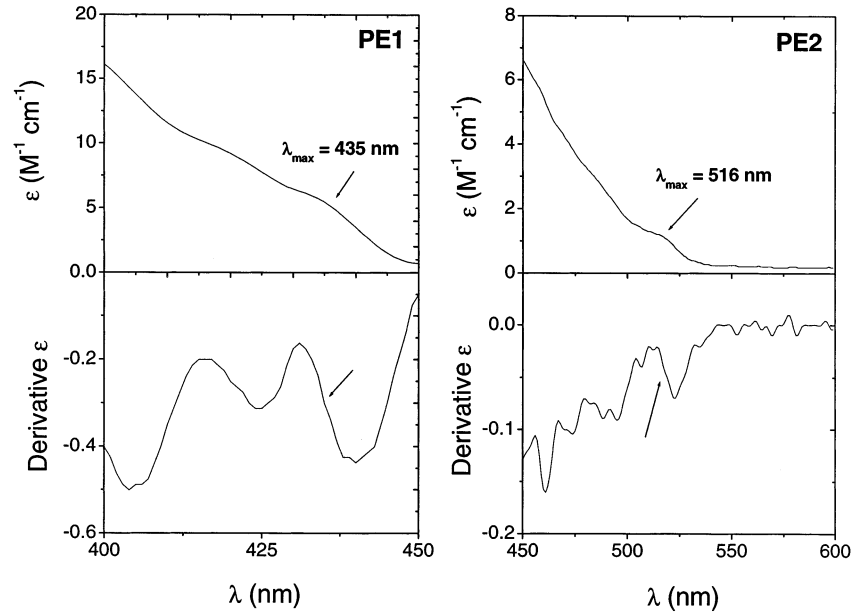

Figure 3. Ground-state absorption spectra of PE1 (1.12 mM) and PE2 (1.12 mM) measured using a long cell spectrometer. Data shown were obtained in benzene at room temperature (25 °C) using a 30 cm path length. The lower panel shows the derivative of the absorption spectrum to help identify the maximum point of the red-shifted shoulder.

co-workers (520 nm) in dichloroethane.[28] For both PPE and PE3 no clear shoulder was observed due to an S_0-T_1 transition.

Fluorescence and Phosphorescence. Figure 2 also shows the emission spectra for each of the oligomers after removal of oxygen by three freeze−pump−thaw cycles. In the case of PE1 very little emission is observed at room temperature. Using a high concentration of PE1 (0.001 12 M) and front face geometry an air-saturated emission spectrum was obtained at room temperature. A small peak at 365 nm is due to S_1-S_0 emission of PE1 and has been amplified (x40) for clarity in Figure 2. For PPE, PE2, and PE3 the maxima at 390, 395, and 400 nm, respectively, are due to emission from S_1-S_0. The fluorescence has been amplified for clarity relative to the phosphorescence peak. For PE2**,** this is consistent with the literature value of 410 nm in dichloroethane.[28] The more red-shifted bands at 510, 526, and 555 nm for PPE, PE2, and PE3 respectively, are confirmed to be room-temperature phosphorescence from T_1-S_0 because of their enhancement upon the removal of oxygen. The observed room-temperature phosphorescence is typical of platinum-containing compounds.[28−30] Very little room-temperature phosphorescence was observed for PE1. The phosphorescence shown in Figure 2 for PE1 was obtained in methyl-

TABLE 1: Summary of Photophysical Properties of Oligomers in Benzene

	E_S (eV)	E_T (eV)	ΔE_{ST} (eV)	Φ_f	Φ_{ISC}	Φ_P[a]
PE1	3.58	2.82	0.76	<0.0006		<0.0001
PPE	3.40	2.58	0.82	0.010	0.60 ± 0.09	0.235
PE2	3.29	2.38	0.91	0.001	0.92 ± 0.08	0.154
PE3	3.21	2.26	0.95	0.016	0.74 ± 0.11	0.017

[a] Measured at room temperature following oxygen removal by freeze−pump−thaw.

TABLE 2: Rate Constants for Decay from the Triplet Excited State

	τ_T	k_p (s^{-1})	k_{nr} (s^{-1})[d]
PE1	590 ± 150 ps[a]	$\sim 1.7 \times 10^{5}$[c]	$\sim 1.7 \times 10^{9}$[c]
PPE	11 ± 1 μs[b]	3.6×10^{4}	5.5×10^{4}
PE2	42 ± 1 μs[b]	4.0×10^{3}	2.0×10^{4}
PE3	86 ± 2 μs[b]	2.7×10^{2}	1.2×10^{4}

[a] Measured in air-saturated benzene using picosecond pump−probe spectroscopy. [b] Oxygen removed from benzene by three successive freeze−pump−thaw cycles. [c] Assuming $\Phi_{ISC} = 1$. [d] Rate constant of nonradiative decay measured using $k_T = k_p + k_{nr}$.

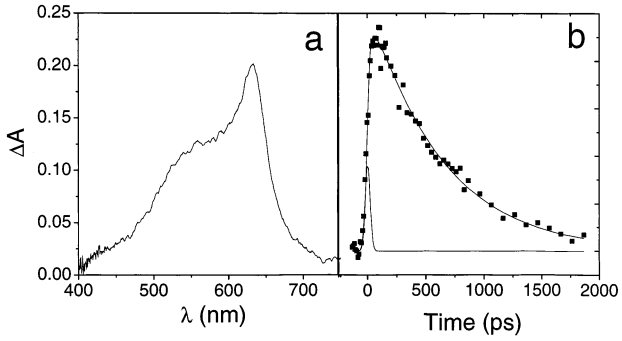

Figure 4. (a) Transient spectrum observed 105 ps after a ca. 30 ps pulsed 355 nm excitation of PE1 (312 μM) in air-saturated benzene. (b) Single-exponential decay of the triplet excited state at 630 nm. Also shown is the instrument response function of the picosecond pump−probe system. Data were fit to a deconvolution model to obtain decay rate constants.

cyclohexane at 77 K. The small peak at room temperature that overlaps with the low temperature data is attributed to room temperature phosphorescence. The slight red shift is most likely due to solvent and temperature effects. Shown in Table 1 are the O−O singlet and triplet excited-state energies (E_S and E_T) for each of the oligomers that were determined from the crossing point of the absorbance and emission spectra.

The fluorescence quantum yields were determined for each of the oligomers according to the method of relative actinometry. These values are given in Table 1 for the oligomers and are all relatively small (<2%). This would be expected due to the heavy atom effect of the platinum metal to induce intersystem crossing to the triplet excited state. We also measured the phosphorescence quantum yields at room temperature in benzene and these are given in Table 1. The yields obtained are fairly significant under deoxygenated room-temperature conditions. The decay rate constants for phosphorescence (k_p), calculated using eq 6, are shown in Table 2. A clear trend is observed that the rate of phosphorescence decay becomes smaller with increased conjugation length.

T_1-T_n Properties. Figure 4 shows the transient spectrum observed 105 ps after 355 nm excitation (ca. 30 ps pulse) of PE1 in air-saturated benzene. The identity of the transient was determined to be that of the triplet excited state of PE1 by use of a triplet sensitization experiment. Using the nanosecond laser flash photolysis experiment, we observe a transient that is

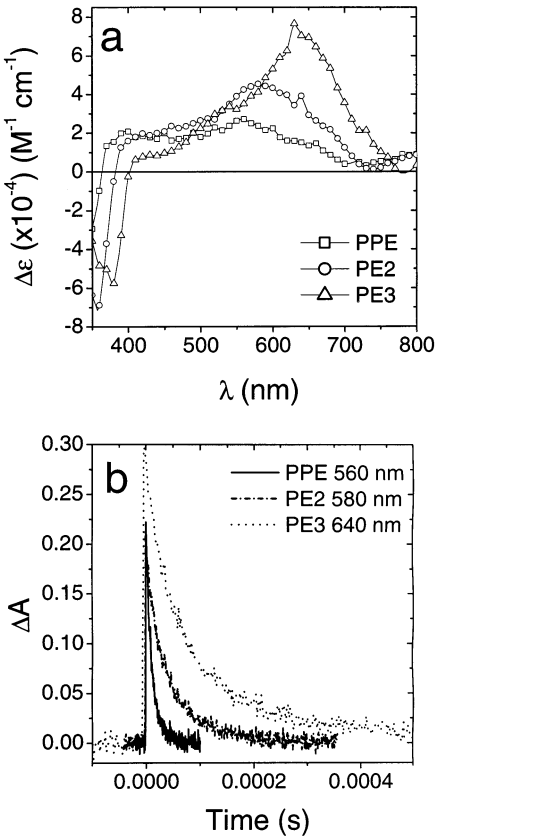

Figure 5. (a) T_1-T_n absorption spectra observed after nanosecond pulsed 355 nm excitation of PPE (12.9 μM), PE2 (4.5 μM), and PE3 (5.2 μM) in argon-saturated benzene. Molar absorption coefficients were obtained using the methods of triplet sensitization and singlet depletion as described in the text. (b) Shown are the single-exponential decays of the triplet excited state obtained after three freeze−pump−thaw cycles to remove oxygen.

formed and decays within the laser pulse (ca. 15 ns) that is identical to that observed in the picosecond experiment. A sensitization experiment was done to test if this transient is due to the triplet excited state of PE1. Using the nanosecond laser flash photolysis experiment, we directly excited PE1 to the triplet excited state and monitored the formation of a transient due to the triplet excited state of β-carotene. Production of the β-carotene triplet is evidence that the short-lived species is the triplet excited state of PE1. To be certain that the β-carotene was not being directly excited ($\phi_{ISC} = <0.001$),[24] a sample of the same concentration without PE1 was excited at 355 nm and we found no production of the triplet excited state. Shown in Figure 4b is the decay of the PE1 triplet excited state measured using the picosecond experiment. The lifetime of this species in air-saturated benzene is 590 ± 150 ps. Due to the short-lived species we were unable to quantify the molar extinction coefficient of PE1. Shown in Figure 5a are the differential spectra obtained upon 355 nm nanosecond excitation of PPE, PE2, and PE3. The identities of the transients were confirmed by molecular oxygen quenching of the excited state and also by energy transfer to β-carotene in the sensitization experiments. The T_1-T_n molar extinction coefficients were determined using both an energy transfer sensitization technique and a singlet depletion method. The values determined for both methods are within error of each other (PPE $\epsilon_{560nm} = 26\,500 \pm 4000$ M^{-1} cm^{-1}, PE2 $\epsilon_{580nm} = 45\,000 \pm 3800$ M^{-1} cm^{-1}, and PE3 $\epsilon_{640nm} = 72\,000 \pm 10\,900$ M^{-1} cm^{-1}). The T_1-T_n spectrum obtained for PE2 is consistent with that found by McKay et al.[31] The T_1-T_n molar extinction coefficient ($\epsilon = 57\,200$ M^{-1} cm^{-1}) is

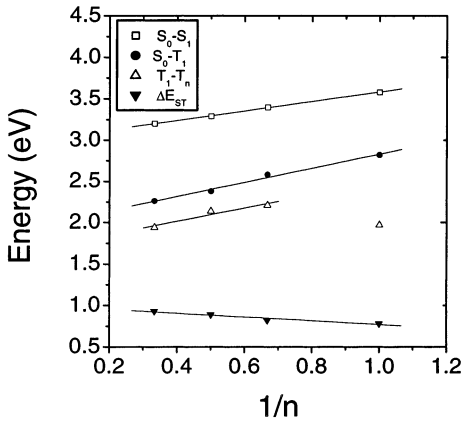

Figure 6. Plot of the E_S, E_T, T_1-T_n (peak max), and ΔE_{ST} (splitting of the singlet and triplet energies) vs 1/*n*, where *n* is defined as the effective conjugation length of the phenyl ethynyl group where PE1 is 1, PPE is 1.5, PE2 is 2, and PE3 is 3.

slightly higher than the value we determined, which is likely due to solvent effects (dichloroethane vs benzene). For PPE, PE2, and PE3 it was found that as the conjugation increases, the intensity of the peak maximum increases and red shifts.

In an attempt to measure the singlet-state lifetimes of these compounds picosecond pump−probe experiments were done. As mentioned earlier, we were able to monitor the decay of the triplet excited state of PE1 with this experiment (Figure 4). For all of the compounds we observed direct formation of the triplet excited state within the laser pulse (ca. 30 ps). Therefore, we can set an upper limit on the singlet-state lifetimes (τ_s) of <30 ps corresponding to a decay rate constant of $>3.3 \times 10^{10}$ s^{-1}.

Shown in Figure 5b are examples of the decay of the triplet excited state for PPE, PE2, and PE3. The decays were fit to a first-order exponential decay model. The triplet excited-state lifetimes (τ_T) are given in Table 2. These lifetimes were obtained by deoxygenating the samples three successive times by freeze−pump−thaw. A clear trend is observed that as the conjugation increases the lifetime gets longer. The quantum yields for intersystem crossing were determined for PPE, PE2, and PE3 in benzene. The values are given in Table 1.

Discussion

Metal-containing π-conjugated systems are attractive molecules for use in materials science. These compounds are easily altered by varying the metal or the ligand, providing tunability of both photophysical and redox properties. The series of platinum phenyl−ethynyl chromophores studied in our laboratory have unique photophysical characteristics that can be divided into two categories. These are the effect of increasing the length of the ligand, and thus increasing the overall conjugation, and the role of the metal on the photophysical properties when conjugation is increased.

Effect of Increasing Ligand. Increasing the chain length of the ligand resulted in an overall red shift in the S_0-S_1 absorption, S_0-T_1 absorption, and the T_1-T_n absorption and a lowering in the respective energies. This is shown in Figure 6 where the energies are plotted as a function of 1/(effective conjugation length) (n = number of phenyl−ethynyl units). For S_0-S_1 and T_1-T_n we observed an increase in the molar absorption coefficient by increasing the length of the π-system. On the basis of the red shift observed, it is clear that these transitions involve the conjugated ligands. The S_0-S_1 electronic transition is believed to originate from π(C≡CR) to π^*(C≡CR) orbitals that possess some charge-transfer character based on ground-state molecular orbital calculations for PE1.[32] It has been suggested in the literature that the electronic transition is a result of mixing between the π^*(C≡CR) and empty platinum p-orbitals.[33] Calculations and experimental evidence on a similar series of compounds determined that hybridization occurs between the metal d orbitals and the p_z orbitals of the ligands, which strongly modifies the optical response of the conjugated chains.[34−36] To better understand the nature of the S_0-S_1, S_0-T_1, and T_1-T_n transitions of PE1, PPE, PE2, and PE3 and confirm the previously determined results, time-dependent DFT calculations are currently being done to assign the orbitals responsible for the optical transitions.

For PE1 we observed a triplet excited state that is further red-shifted than the other T_1-T_n spectra (Figure 4). This red shift indicates the character of the T_1-T_n transition is different for PE1. Excitation is at 355 nm in both experiments, which for PE1 occurs on the red edge of the S_0-S_1 transition. Scans of phosphorescence emission both from our own measurement and others[37] show a small shift, $<2-4$ nm, with excitation wavelength, indicating the possibility that the transition that occurs is dependent on excitation wavelength. However, the location of the T_1-T_n peak in PE1 is shifted by a much larger amount, ≈60 nm, than expected from the trends found in the other oligomers. We feel that the nature of the triplet excited state for PE1 is different than that found for the other oligomers but it is clear that the S_0-S_1 and S_0-T_1 transitions follow the expected trends and originate from similar types of states as PPE, PE2, and PE3. This is also evident by comparing the similar slopes of the linear fits for the data in Figure 6. From this it is shown that the PE1 T_1-T_n transition must occur from a different type of state.

Also shown in Figure 6 is a plot of the respective singlet−triplet splittings for each compound. The ΔE_{ST} is plotted as a function of 1/effective conjugation length (n = number of phenyl−ethynyl units). The trend found is that as the conjugation increases the singlet−triplet gap becomes larger. This is the opposite of a study done on a series of linear polyacenes.[38] They found that the singlet triplet gap decreases as the polyacene molecule becomes more conjugated. This phenomenon is correlated to particle in a box theory.[39] The ΔE_{ST} is determined by the exchange integral (2K), which is the sum of all the repulsions and attractions of two overlap charge densities. For a small box there is a greater repulsion from the charge densities being forced into a small box, resulting in a large exchange integral and thus a large ΔE_{ST}. Conversely, if the box is large, then ΔE_{ST} is small because of less repulsion. In the case of the polyacenes, where no charge transfer occurs, as the chain length becomes larger, then the ΔE_{ST} becomes smaller. Therefore the effect of the conjugation on the polyacene must increase the length of the box and thus have less overlap of the charge densities because the LUMO and/or HOMO for the $\pi-\pi^*$ transition is more delocalized over the whole molecule. In a separate study on a series of platinum-containing monomers and polymers with varying chain lengths, it was determined that the S_1 energy is raised more than the T_1 energy when going from a polymer to its corresponding monomer, and as a result, the ΔE_{ST} is larger for the monomer than for its polymer.[40] They conclude that in the case of the monomers that the triplet exciton is more spatially localized where the singlet exciton tends to be more extended over the molecule. This is because the electrons are better correlated via the exchange interaction in the triplet state than in the singlet state. Therefore the ΔE_{ST} is larger for the monomer than its polymer. Again this is the opposite finding of our data because in the case of our

compounds we observed an increase in ΔE_{ST} with increased ligand length. Another separate theoretical study on a series of oligothiophenes, where the chain length was varied from 1 to 6 thiophene units, resulted in a decrease in ΔE_{ST} with extension of the chain length.[41] In this paper they show a plot of the S_0-S_1 and S_0-T_1 energies as a function of $1/n$, which is what is shown in Figure 6 for our data. They determined that the slope of the S_0-T_1 data resulted in a weak evolution of the lowest triplet excitation energy that reflects the strong confinement of the triplet exciton. The S_0-S_1 slope is relatively large, which indicates a more delocalized singlet exciton. Comparing the slopes of S_0-S_1 and S_0-T_1 in Figure 6, the slope of the S_0-T_1 data is slightly larger than that of the S_0-S_1 data. We interpret this finding to mean that the triplet exciton may be more delocalized than the singlet exciton, although the slopes of these two lines are very similar and the extent of delocalization may be minimal. This finding accounts for the differences in the ΔE_{ST} of our data and the other three studies presented.

Effect of Platinum on Increasing Ligand Length. To explore the effect of the metal on the oligomers, we tried to assess the influence of spin−orbit coupling on the photophysical properties. It is known[38] that the limiting parameters for the extent of spin−orbital coupling that occur are the spin−orbit coupling constant of the heavy atom and the extent of penetration of the electrons of the molecular skeleton into the field gradient of the heavy atom. Because this series of compounds all contain platinum, the spin−orbit coupling constant should be most affected by distance. It is proposed that as the ligand length increases, the S_0-S_1 transition is more localized on the conjugated ligand, taking on more $\pi-\pi^*$ character, and therefore is spatially further away from the platinum center, thus reducing spin−orbit coupling. The photophysical properties shown in Table 1 support this proposed idea. It has been reported by McGlynn, Azumi, and Kinoshita in *Molecular Spectroscopy of the Triplet State*[39] that an increase in spin−orbit coupling alters the photophysical processes such that the following are observed:

(1) an enhancement of S_0-T_1 absorption

(2) an increase in phosphorescence quantum yield (Φ_P)

(3) a decrease in the radiative lifetime of phosphorescence, which corresponds to a decrease in the triplet excited-state lifetime

(4) a decrease in fluorescence quantum yield (Φ_f)

(5) an increase in the rate constant of intersystem crossing (k_{ISC})

Each of these effects, and how they relate to our series of compounds, will be discussed in further detail below.

(1) Enhancement of S_0-T_1. For the oligomers we observed a decrease of the S_0-T_1 extinction coefficient as the conjugation length increased (Figure 3). The weak absorption bands are observed using a long path length spectrometer and the molar extinction coefficients measured are below 5 M^{-1} cm^{-1}. For PE1 and PE2 a small peak is observed that correlates well with the room-temperature phosphorescence data. In the case of PPE and PE3 we could not clearly identify the S_0-T_1 peak. For PE1 and PE2 it appears that a decrease in the extinction coefficient is observed as well as a red shift in the peak maximum with increased conjugation.

(2) Increase in Φ_P. The phosphorescence quantum yields were measured for the oligomers in deoxygenated room-temperature benzene and are given in Table 1. For PPE, PE2, and PE3 we observed room-temperature phosphorescence that increased upon removal of oxygen. Comparing the quantum yields measured, it is clear that as the chain length becomes longer, the phosphorescence yield is smaller. For PE1 we did not observe any phosphorescence following deoxygenation. We assume that the quantum yield for phosphorescence is <0.0001 and that nearly all the triplets formed deactivate through a more competitive internal conversion pathway (k_{nr} shown in Table 2).

(3) Decrease in k_p. The third point states that the phosphorescence lifetime decreases with an increase in spin−orbit coupling. This is shown in Table 2. This trend correlates well, supporting that spin−orbit coupling is reduced with longer ligand chain length. Another indication that spin−orbit coupling decreases with increased conjugation is a comparison of the triplet excited-state lifetimes (Table 2). With increasing overlap of the empty metal orbitals with the π orbitals and increasing spin−orbit coupling, the spin selection rules are weakened, leading to a significant increase of allowedness, and thus to a decrease of the triplet lifetime.[42] We find that as the conjugation increases, the lifetimes become longer. The magnitude of the triplet excited-state lifetime depends on the orbitals involved in the electronic transition, the nuclear configuration of the initial and final states, and the extent of spin−orbit coupling in the triplet state.[27] The major factor is generally the spin−orbit term. We observe a dramatic increase in the lifetimes from 590 ps to 86 μs for PE1 and PE3**,** respectively, suggesting that PE1 is affected the greatest by spin−orbit coupling and possesses the most metal character.

(4) Decrease in Φ_F. Comparing the small fluorescence quantum yields of the oligomers (Table 1) yields a trend for PE1, PE2, and PE3. There is a correlation between the fluorescence quantum yield and the singlet triplet energy splitting, ΔE_{ST}, shown in Table 1. As the splitting becomes larger, we observe an increase in the fluorescence quantum yield. PPE has an anomalously large fluorescence quantum yield compared to the others of comparable ligand length. This difference is rationalized because the biphenyl part of the ligand is different from the phenyl linkages of the other oligomers. PPE does not strictly fit into this series of oligomers.

(5) Increase in k_{ISC}. The last point is that an increase in the rate constant for intersystem crossing should be observed, but unfortunately, we were not able to measure this rate. We know from the picosecond pump−probe experiments that the triplet excited state was formed within the 30 ps laser pulse for all species. This puts a lower limit on the decay of the singlet excited state of $k_s > 3.3 \times 10^{10}$ s^{-1}. The ability for intersystem crossing to compete effectively with other processes relies on three factors: (1) differing degrees of electronic coupling between S_1 and the triplet state to which crossing occurs, (2) differing energy gaps between S_1 and the triplet state to which crossing occurs, and (3) differing degrees of spin−orbit coupling between S_1 and the triplet state to which crossing occurs.[27] On the basis of the ΔE_{ST} measured and the theory that spin−orbit coupling is less effective for the longer length oligomers, and on the basis of the above-mentioned evidence, we expect that the rate for intersystem crossing and in turn the quantum yields for intersystem crossing to be smaller as the conjugation length increases. For PE1 we were unable to measure the quantum yield for intersystem crossing. We believe that PE1 has a considerably fast rate of intersystem crossing leading to a large Φ_{ISC} because it has the smallest singlet−triplet splitting. Comparing the values of Φ_{ISC} in Table 1 and assuming that Φ_{ISC} for PE1 is nearly unity, then a trend is observed that Φ_{ISC} becomes smaller as the chain length becomes longer. PPE has a smaller quantum yield than expected but this may be due to the differences in the ligand (biphenyl vs phenyl).

Conclusions

The trends observed for this series of transition metal-containing phenylacetylenes provides an understanding of the photophysical trends inherent in this type of chromophore. It was learned that by extending the π-conjugated ligand an overall red shift in the ground-state and excited-state absorption and an increase in the molar absorption coefficient was observed. As the conjugation length increases, an increase is observed in the ΔE_{ST} that results in a believed slower rate for intersystem crossing, thus leading to a smaller triplet quantum yield. Also with increased conjugation the triplet excited-state lifetime becomes longer, which is proposed to be due to the spin−orbit coupling effect being reduced. Future directions of this research include synthesizing polymeric forms of these dyes and studying their photophysical properties.

Acknowledgment. We are grateful for the support of this work by AFRL/ML contracts F33615-99-C-5415 for D.G.M. and F33615-97-D-5405 for J.E.R. We thank Prof. Bradley Arnold and Dustin Levy, University of Maryland Baltimore County, for use of their picosecond pump−probe system.

References and Notes

(1) Nalwa, H. S. *Handbook of Organic Conductive Molecules and Polymers*; John Wiley & Sons: Chichester, U.K., 1997; Vols. 1−4.
(2) Skotheim, R. A.; Elsenbaumer, R. L.; Reunolds, J. R. *Handbook of Conducting Polymers*, 2nd ed.; Marcel Dekker: New York, 1998.
(3) Patil, A. O.; Heeger, J.; Wudl, F. *Chem. Rev.* **1988**, *88*, 183−200.
(4) Burroughes, J. H.; Bradley, D. D. C.; Brown, A. R.; Marks, R. N.; Mackay, K.; Friend, R. H.; Burns, P. L.; Holmes, A. B. *Nature* **1990**, *347*, 539.
(5) Brown, A. R.; Pichler, K.; Greenham, N. C.; Bradley, D. D. C.; Friend, R. H.; Holmes, A. B. *Chem. Phys. Lett*. **1993**, *210*, 61.
(6) Tessler, N.; Denton, G. J.; Friend, R. H. *Nature* **1996**, *382*, 695.
(7) Donhauser, Z. J.; Mantooth, B. A.; Kelly, K. F.; Bumm, L. A.; Monnell, J. D.; Stapleton, J. J.; Price Jr, D. W.; Rawlett, A. M.; Allara, D. L.; Tour, J. M.; Weiss, P. S. *Science* **2001**, *292*, 2303.
(8) Yam, V.; Lo, K.; Wong, K. *J. Organomet. Chem*. **1999**, *578*, 3.
(9) Nguyen, P.; Gomez-Elipe, P.; Manners, I. *Chem. Rev.* **1999**,*99*, 1515.
(10) Ley, K. D.; Schanze, K. S. *Coord. Chem. Rev*. **1998**, *171*, 287.
(11) Yang, M.; Ziqiang, L.; Cai, Z. *Polymer* **1999**, *40*, 3203.
(12) Yang, M.; Ziqiang, L.; Wan, M.; Shen, Y.; Wang, J.; Chen, J.; Wang, H.; Ye, T. *J. Appl. Polym. Sci*. **1997**, *64*, 1657.
(13) Walters, K. A.; Ley, K. D.; Cavalaheiro, C.; Miller, S. E.; Gosztola, D.; Wasielewski, M.; Bussandri, A. P.; van Willigen, H.; Schanze, K. S. *J. Am. Chem. Soc*. **2001**, *123*, 8329.
(14) Li, Y.; Whittle, C. E.; Walters, K. A.; Ley, K. D.; Schanze, K. S. *Pure Appl. Chem.* **2001**, *73*, 497.
(15) Wittmann, H. F.; Friend, R. H.; Khan, M. S.; Lewis, J. *J. Chem. Phys*. **1994**, *101*, 2693.
(16) McKay, T. J.; Bolger, J. A.; Staromlynska, J.; Davy, J. R. *J. Chem. Phys*. **1998**, *108*, 5537.
(17) Kaufmann, G. B.; Teter, L. A. *Inorg. Synth.* **1963,** *VII*, 245.
(18) Lavastre, O.; Ollivier, L.; Dixneuf, P. *Tetrahedron* **1996,** *52*, 5495.
(19) Sonogashira, K.; Fujikura, Y.; Yatake, T.; Toyoshima, N.; Takahashi, S.; Higihara, N. *J. Organomet. Chem.* **1978** *145*, 101.
(20) Demas, J. N.; Crosby, G. A. *J. Phys. Chem*. **1971**, *75*, 991.
(21) Poliakov, P.; Arnold, B. R. *Spectrosc. Lett*. **1999**, *32*, 747.
(22) The value listed for β-carotene was measured in benzene using the triplet sensitization technique employing *meso*-tetraphenylporphine as an energy donor. ($\epsilon_{790nm} = 6000\ M^{-1}\ cm^{-1}$): Lee, W. A.; Graetzel, M.; Kalyanasundaram, K. *Chem. Phys. Lett*. **1984**, *107*, 308.
(23) Charmichael, I. Helman, W. P.; Hug, G. L. *J. Phys. Chem. Ref. Data* **1987**, *16*, 239.
(24) Bensasson, R.; Dawe, E. A.; Long, D. A.; Land, E. J. *J. Chem. Soc., Faraday Trans. 1*, **1977**, *73*, 1319.
(25) Carmichael, I.; Hug, G. *J. Phys. Chem. Ref. Data* **1986**, *15*, 1.
(26) Cooper, T. M.; McLean, D. G.; Rogers. J. E. *Chem. Phys. Lett*. **2001**, *349*, 31.
(27) Turro, N. J. *Modern Molecular Photochemistry*; University Science Books: Sausalito, CA, 1991.
(28) Staromlynska, J.; McKay, R. J.; Bolger, J. A.; Davy, J. R. *J. Opt. Soc. Am. B* **1998**, *15*, 1731.
(29) Hissler, M.; Connick, W. B.; Geiger, D. K.; McGarrah, J. E.; Lipa, D.; Lachicotte, R. J.; Eisenberg, R. *Inorg. Chem*. **2000**, *39*, 447.
(30) Whittle, C. E.; Weinstein, J. A.; George, M. W.; Schanze, K. S. *Inorg. Chem*. **2001**, *40*, 4053.
(31) McKay, T. J.; Staromlynska, J.; Davy, J. R.; Bolger, J. A. *J. Opt. Soc. Am. B* **2001**, *18*, 358.
(32) Younus, M.; Long, N. J.; Raithby, P. R.; Lewis, J. *J. Organomet. Chem*. **1998**, *570*, 55.
(33) Masai, H.; Sonogashira, K.; Hagihara, N. *Bull. Chem. Soc. Jpn*. **1971**, *44*, 2226.
(34) Beljonne, D.; Wittmann, H. F.; Kohler, A.; Graham, S.; Younus, M.; Lewis, J.; Raithby, P. R.; Khan, M. S.; Friend, R. H.; Bredas, J. L. *J. Chem. Phys*. **1996**, *105*, 3868.
(35) Chawdhury, N.; Kohler, A.; Friend, R. H.; Wong, W. Y.; Lewis, J.; Younus, M.; Raithby, P. R.; Corcoran, T. C.; Al-Mandhary, M. R. A.; Khan, M. S. *J. Chem. Phys*. **1999**, *110*, 4963.
(36) Younus, M.; Kohler, A.; Cron, S.; Chawdhury, N.; Al-Mandhary, M. R. A.; Khan, M. S.; Lewis, J.; Long, N. J.; Friend, R. H.; Raithby, P. R. *Angew. Chem., Int. Ed. Engl.* **1998**, *37*, 3036.
(37) Sacksteder, L.; Baralt, E.; DeGraff, B. A.; Lukehart, C. M.; Demas, J. N. *Inorg. Chem*. **1991**, *30*, 2468.
(38) McGlynn, S. P.; Smith, F. J.; Cilento, G. *Photochem. Photobiol*. **1964**, *3*, 269.
(39) McGlynn, S. P.; Azumi, T.; Kinoshita, M. *Molecular Spectroscopy of the Triplet State*; Prentice-Hall: Englewood Cliffs, NJ, 1969.
(40) Kohler, A.; Wilson, J. S.; Friend, R. H.; Al-Suti, M. K.; Khan, M. S.; Gerhard, A.; Bassler, H. *J. Chem. Phys*. **2002**, *116*, 9457.
(41) Bredas, J. L.; Cornil, J.; Meyers, F.; Beljonne, D. *Handbook of Conducting Polymers*, 2nd ed.; Marcel-Dekker: New York, 1998; pp 1−25.
(42) Yersin, H.; Humbs, W. Strasser, J. *Coord. Chem. Rev*. **1997**, *159*, 325.